Chemical Engineering Journal 154 (2009) 333–340

Contents lists available at ScienceDirect

Chemical Engineering Journal

journal homepage: www.elsevier.com/locate/cej

NH_3-SCR on Fe zeolite catalysts – From model setup to NH_3 dosing

A. Schuler[a,*], M. Votsmeier[b], P. Kiwic[c], J. Gieshoff[b], W. Hautpmann[b], A. Drochner[a], H. Vogel[a]

[a] Ernst-Berl-Institute, TU-Darmstadt, Petersenstr. 20, 64287 Darmstadt, Germany
[b] Umicore AG & Co. KG, Rodenbacher Chaussee 4, 63457 Hanau, Germany
[c] Institute for Measurement and Control, ETH Zürich, Sonneggstr. 3, 8092 Zuerich, Switzerland

ARTICLE INFO

Article history:
Received 10 December 2008
Received in revised form 21 February 2009
Accepted 24 February 2009

Keywords:
Fe exchanged zeolite
SCR
NH_3
Ammonia
NH_3 dosing
Control
Standard SCR Reaction
Fast SCR Reaction
NO_2 SCR Reaction

ABSTRACT

The setup of a detailed model for the NH_3-SCR process on iron exchanged zeolite catalysts is described, which takes into account the reactions of NH_3, NO and NO_2 occurring under typical exhaust conditions. Validation experiments for a standard SCR gas mixture show that the model is able to describe the dynamic behaviour of this system at transient temperature conditions. The model is used for the parameterization of an ammonia dosing controller. To prove the functionality of this controller it was implemented on a synthetic gas test bench and tested by a dynamic temperature experiment. This setup allows the evaluation of the parameterized controller without any disturbances from engine or injection effects.

1. Introduction

To remove pollutants from the exhaust of diesel engines, several technologies have been developed in the past. One technology for NO_x abatement in vehicles, as well used in combustion processes, is the selective catalytic reduction with ammonia as reducing agent (NH_3-SCR). Around this topic a lot of research efforts have been made to find appropriate catalytic systems and to understand the mechanistic backgrounds of the processes on the catalyst surface. Vanadia-based systems were found to be more effective with WO_3 support [1,2] and metal exchanged zeolites were developed as second generation catalysts [1,3]. A review of Busca gives a comprehensive overview about materials, kinetic studies and proposed mechanisms until 1998 [4]. Concerning Fe exchanged zeolites Chen and Sachtler [5] and Long and Yang were the first to investigate the SCR processes on Fe–ZSM-5 as a model system [6–8].

A lot of kinetic studies and meanwhile kinetic models have been published for several catalysts: Tronconi and Chatterjee et al. [9–11] and Schär et al. for a vanadia-based catalysts [12], we [13,14] as well as Chatterjee et al. [11] for Fe zeolite catalysts and Olsson et al. [15] for copper exchanged zeolites.

One benefit of such a model is its utilization for the parameterization of an ammonia dosing controller as it is used in the vehicle. The controller has to provide the amount of reducing agent necessary at each operation point according to certain a dosing strategy. There are some recent publications about urea dosing and its strategies [16–18]. Usually the required amount of NH3 is determined using look up tables, as a model-based calculation would demand too much processing power for an engine control computer. For the parameterization of the lookup tables, both experimental and model-based methods are possible. As the parameterization by experiments is a time consuming procedure, using a model should be more efficient. On an engine or vehicle test bench the controller performance is influenced by many effects apart from the catalytic system, e.g. misdistribution of injected urea. These effects and the controller performance cannot be separated, thus in terms of method evaluation it is reasonable to test the controller at a synthetic gas test bench. Altogether, this work describes the following issues:

- The setup and validation of a model for a commercial Fe zeolite catalyst. The model has to describe the system having regard to both transient and steady state features of the system.
- Validation of the model with a transient model gas experiment.
- Utilization of the obtained model for parameterizing an ammonia dosing controller in view of its application in the vehicle.

* Corresponding author. Tel.: +49 6181 59 8201; fax: +49 6181 597 8201.
E-mail address: schuler@ct.chemie.tu-darmstadt.de (A. Schuler).

1385-8947/$ – see front matter © 2009 Elsevier B.V. All rights reserved.
doi:10.1016/j.cej.2009.02.037

Nomenclature

E_A	activation energy (J mol^{-1})
GHSV	gas hourly space velocity (h^{-1})
K_{NH_3}	parameter for ammonia inhibition
k_0	pre-exponential factor (mol m^{-3} s^{-1}; s^{-1})
r	rate of reaction (mol m^{-3} s^{-1})
R	ideal gas constant (J mol^{-1} K^{-1})
t	time (s)
T	temperature (K or °C)
x_i	molar ratio of component i
α	dosing ratio, $x(NH_3)$:$x(NO_x)$
β	reaction order of O_2, Standard SCR Reaction
ε	reaction order of O_2, NH_3 oxidation
γ	parameter for surface coverage dependency of NH_3 desorption
Θ	surface coverage of NH_3

- Proving the functionality of the obtained controller by implementation at the synthetic gas test bench.

2. Methods

2.1. Experimental

The SCR model was developed and validated using a commercial monolith sample. The substrate is a cordierite monolith of 400 cpsi with a dimension of 1 in. × 3 in., coated with a mixture of Fe exchanged zeolites. The sample was aged for 200 h at 650 °C and 50 h at 750 °C under hydrothermal conditions. Before the measurements the sample was conditioned at 600 °C for 20 min.

The experiments shown are performed in a quartz reactor with an integrated heat exchanger. The feed gas is a mixture of calibrated gases and was dosed by a set of mass flow controllers. The gas from the outlet of the reactor is analyzed by an FT-IR spectrometer, equipped with a gas cell of 200 mL volume and a path length of 2 m. The analyzer was calibrated for the components NO, NO_2, NH_3 and N_2O, spectra were taken with a time resolution of 1 Hz.

For experiments using the ammonia dosing controller, the laboratory automation of the synthetic gas test bench described above was adapted (Fig. 1). The controller was operated in parallel to the laboratory automation system and from there it got inputs like temperature, gas hourly space velocity (GHSV) and NO concentration. Using these values the dosing controller calculated the optimum amount of ammonia at current conditions and according to this adjusted the setpoint of the ammonia mass flow controller. This situation is similar to the operation in a vehicle, where the inputs come from the engine control computer, and the outputs of the controller are provided to the urea dosing system.

2.2. Simulation program

The model used for simulation is 1D and computes a single channel of the monolith. It regards physical processes like convection in the gas phase, heat and mass transfer between gas phase and wash coat and heat transfer in the substrate as well as chemical reactions. These reactions can occur between gaseous and adsorbed species. The program solves the conservation equations of mass, momentum and energy for gas and solid phase. So the physicochemical model allows a fully transient computation of surface coverage, storage and reaction phenomena, by solving the system of nonlinear partial differential equations.

3. Results and discussion

3.1. Kinetic model setup

The kinetic model described in the following takes in to account the reactions occurring with NH_3, NO and NO_2 under typical gas conditions of lean engine exhaust. Therefore high concentrations of H_2O (5%) and O_2 (6%) were present in the gas feed mixture of each experiment. The kinetic parameters generally were fitted according to both steady state and transient response experiments. The reactions were included in the model consecutively, in the same order they are described in the following.

3.1.1. Ammonia adsorption/desorption

The adsorption and desorption of ammonia according to (R1) was investigated by an NH_3 pulse on a clean surface (preconditioning at 450 °C at 600 ppm NO, 6% O_2, 5% H_2O).

$$NH_3 + [*] \leftrightarrow NH_3* \quad \text{(R1)}$$

The experiment was performed with different concentrations of NH_3 (150–1500 ppm) at temperatures between 175 and 400 °C. The rate equations used for the NH_3 adsorption and desorption are shown in (1) and (2):

$$r_{ads,NH_3} = k_{0,ads} \cdot c_{NH_3} \cdot (1 - \Theta) \quad (1)$$

$$r_{des,NH_3} = k_{0,des} \cdot \exp\left(\frac{-E^{\circ}_{A,des}}{R \cdot T}(1 - \gamma \cdot \Theta)\right) \cdot \Theta \quad (2)$$

The ammonia adsorption is regarded to be a non-activated process. The rate of desorption is covered by an expression according to a Temkin type adsorption isotherm, where the activation energy

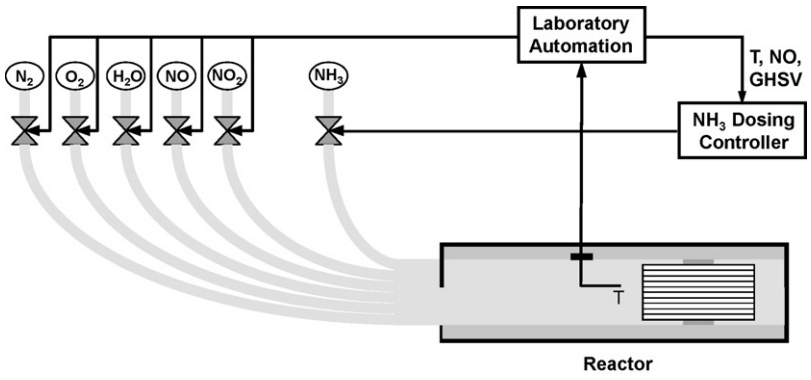

Fig. 1. Scheme of the synthetic gas test bench equipped with the ammonia dosing controller.

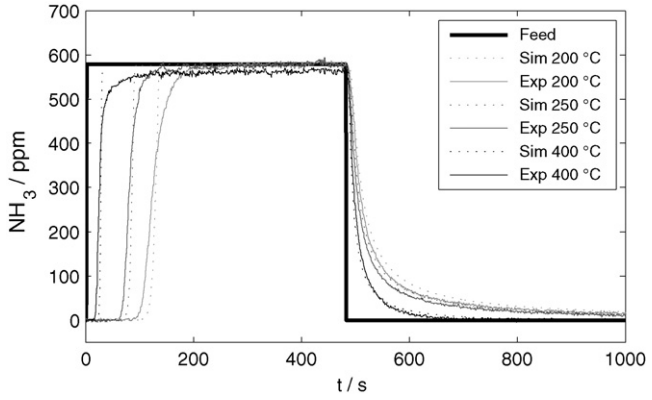

Fig. 2. Simulation and experimental results of the ammonia adsorption and desorption experiment performed at different temperatures (6% O_2, 5% H_2O, GHSV 25,000 h^{-1}).

of desorption is a function of the surface coverage. These rate equations were first used by Tronconi et al. [19] for vanadia-based catalysts and also work quite well for the iron exchanged zeolite system [13,14].

In Fig. 2 experiments and simulations are compared for three temperatures with a feed concentration of NH_3 of 600 ppm. The model is able to reproduce the curves, the desorption process especially is reproduced well. The adsorption curves show deviations near to the complete break through. The experimental curve at 400 °C shows the occurrence of ammonia oxidation, as the dosed value is not reached even at steady state conditions.

3.1.2. Ammonia oxidation

The oxidation of ammonia with oxygen according to (R2) is an undesired side reaction, which occurs at temperatures above 400 °C. Nitrogen is formed selectively at the conditions considered, as no other oxidation products have been found.

$$4NH_3 + 3O_2 \rightarrow 2N_2 + 6H_2O \quad \text{(R2)}$$

This reaction was investigated with steady state experiments at temperatures between 300 and 550 °C. To study the impact of the ammonia feed concentration, one test series was performed at constant O_2 concentration of 6% with a variation of the NH_3 feed (100–1600 ppm). Another series of measurements was made to map the effect of the O_2 concentration (600 ppm NH_3, 3–21% O_2). The results show that oxygen promotes the NH_3 oxidation. The NH_3 conversion falls with rising NH_3 concentration; this reveals a global reaction order <1 for NH_3 in this process. In the model the NH_3 oxidation was regarded according to following rate expression (3):

$$r_{NH_3\text{-Ox}} = k_{0,NH_3\text{-Ox}} \cdot \exp\left(\frac{-E_{A,NH_3\text{-Ox}}}{R \cdot T}\right) \cdot \left(\frac{x_{O_2}}{0.06}\right)^{\varepsilon} \cdot \Theta \quad (3)$$

Oxygen reacts with adsorbed ammonia. The influence of O_2 is taken into account by a power law expression, which is normed to the standard concentration of O_2. The fitted parameters were the Arrhenius constants and the reaction order of oxygen. The fit was performed to the results of the oxygen variation. In Fig. 3 simulation and experimental results are illustrated.

3.1.3. NO oxidation

In contrast to vanadia-based catalyst systems, iron exchanged zeolites are active in terms of NO/NO_2 equilibration [4,11].

$$NO + 0.5O_2 \leftrightarrow NO_2 \quad (3)$$

As NO_2 reacts in other reaction paths as NO, this process has to be taken into account for a model which is able to map the

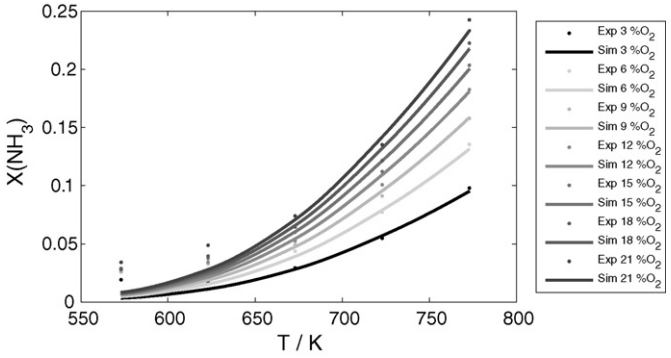

Fig. 3. Simulation and experimental results of the ammonia oxidation performed at different O_2 concentrations (600 ppm NH_3, 5% H_2O, GHSV 25,000 h^{-1}).

NH_3-SCR reactions of NO_x. The oxidation of NO was investigated at temperatures between 150 and 450 °C and different NO feed concentrations (400–1000 ppm NO, 6% O_2, 5% H_2O). The equilibrium concentrations were never achieved, the maximum conversion was 18%.

The experimental results could well be reproduced using rate equation (4), which was also used by Hauptmann et al. for NO oxidation on Pt/Al_2O_3 [20].

$$r_{NO\text{-Ox}} = k_{0,NO\text{-Ox}} \cdot \exp\left(\frac{-E_{A,NO\text{-Ox}}}{R \cdot T}\right) \cdot \left(x_{NO} \cdot x_{O_2}^{0.5} - \frac{x_{NO_2}}{K_{eq}}\right) \quad (4)$$

The rate of the reaction is determined by the offset from the thermodynamic equilibrium. The model was fitted to the measurements with 600 ppm NO in the feed gas. The other experiments served as validation data. Fig. 4 shows the NO emissions according to experiments and simulations of both fitting and validation experiments.

3.1.4. Fast SCR Reaction

The so-called Fast SCR Reaction describes the fast reaction taking place when NO and NO_2 are both present in the feed gas (R4).

$$4NH_3 + 2NO + 2NO_2 \rightarrow 4N_2 + 6H_2O \quad \text{(R4)}$$

As the reaction reaches full conversion at the standard space velocity of 25,000 h^{-1}, this reaction was investigated at higher volume flows adequate to GHSV of 50,000–200,000 h^{-1}. The reaction was performed at temperatures between 150 and 500 °C, the feed concentration of NO and NO_2 were 300 ppm with 600 ppm of NH_3 (5% H_2O, 6% O_2).

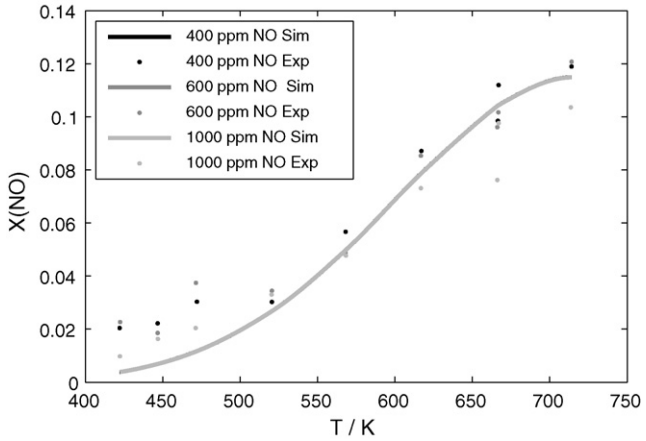

Fig. 4. Simulation and experimental results of the NO oxidation performed at different NO concentrations (400–1000 ppm NO, 6% O_2, 5% H_2O, GHSV 25,000 h^{-1}). All simulated NO curves are superposed, therefore there is just one curve apparent.

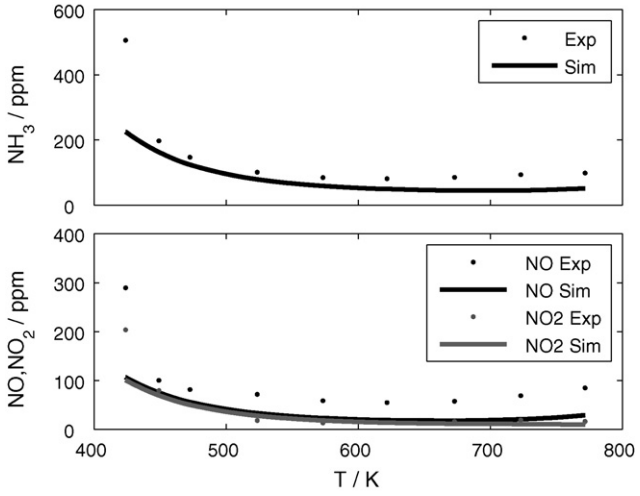

Fig. 5. Simulation and experimental results of the Fast SCR Reaction (300 ppm NO and NO_2, 600 ppm NH_3, 6% O_2, 5% H_2O, GHSV 100,000 h^{-1}).

As there was no evidence of ammonia inhibition at temperatures above 200 °C seen in transient response experiments (not shown here), the rate of the Fast SCR Reaction was covered in an expression according to an Eley–Rideal mechanism (5), where NO and NO_2 react as gas phase species with adsorbed ammonia.

$$r_{\text{fastSCR}} = k_{0,\text{fastSCR}} \cdot \exp\left(\frac{-E_{\text{A,fastSCR}}}{R \cdot T}\right) \cdot c_{\text{NO}} \cdot c_{\text{NO}_2} \cdot \Theta \quad (5)$$

Fig. 5 shows experimental and simulation results. The experimentally observed ratio of NO/NO_2 consumption does not show the stoichiometry of 1/1 implied by (R4). The fraction of converted NO_2 is higher. This phenomenon was also seen by Schwidder et al. [21] and by Grossale et al. [22], who assumed a parallel occurring NH_4NO_3 formation and decomposition to N_2O. We have confirmed this effect on a second test bench, which was calibrated independently.

A parallel NO_2 SCR Reaction can be excluded, because the observed stoichiometry of converted NH_3:NO_x is strictly 1:1. The excess NO_2 conversion in this case would give an higher NH_3 conversion and therefore a stoichiometry higher than NH_3:NO_x = 1:1. Also, the NO/NO_2 equilibrium does not play a major role. An experiment with GHSV 100,000 h^{-1} and NO/NO_2 = 1:1 shows an NO_2 reduction of just 3% at 500 °C (results not shown here).

Grossale et al. [23] discuss a cycle mechanism of the Fast SCR Reaction on Fe zeolite catalysts, in which formation of NH_4^+ and NO_3^- is followed by a reaction with NO to form NO_2, H_2O and N_2 (Fig. 6). This alone cannot explain this phenomenon at real steady state conditions, because at high temperatures NH_4^+ and NO_3^- or NH_4NO_3, respectively would have to accumulate on the surface. If some of the formed NH_4NO_3 took one of the decay paths, either to N_2O and H_2O or even to N_2, O_2 and H_2O (painted in grey, as it is not included in Grossales mechanism), the excess NO_2 conversion could be explained. The decomposed NH_4NO_3 would not be available for NO reaction, and each unit of decomposed NH_4NO_3 would cause an excess conversion of two units NO_2 compared to NO. In consequence there was as much NH_3 converted as NO_x (the exact stoichiometry of NH_3/NO_x = 1:1 was observed for all temperatures), but less NO than NO_2.

At temperatures above 250 °C one observes constant N_2O formation of 11 ppm, this would explain a deviation of NO/NO_2 of 22 ppm. We actually see around 40 ppm more NO_2 converted than NO. Therefore the decomposition to N_2O seems to be the most reasonable decay path. The direct composition to N_2, O_2 and H_2O and even the further reaction of N_2O with ammonia can neither be confirmed nor be excluded because of measuring accuracy constraints. Devadas et al. [24] observed N_2O decomposition at Fe–ZSM-5 above 450 °C, which in combination with NH_4NO_3 decay to N_2O would result in the upper path marked in grey in Fig. 6. It is also known that the presence of NO enhances the reaction of N_2O and NH_3 [27], so that also this reaction probably takes place.

3.1.5. NO_2 SCR Reaction

According to the NO_2 SCR Reaction NH_3 and NO_2 react to form nitrogen and water (R5).

$$8NH_3 + 6NO_2 \rightarrow 7N_2 + 12H_2O \quad (R5)$$

The reaction was investigated by steady state experiments with 600 ppm NH_3 and 450 ppm NO_2 (5% H_2O, 6% O_2) at GHSV of 25,000 and 50,000 h^{-1}. In analogy to the Fast SCR Reaction, an Eley–Rideal mechanism was assumed for the NO_2 SCR Reaction. In this case gaseous NO_2 reacts with adsorbed ammonia (6).

$$r_{\text{NO}_2\text{-SCR}} = k_{0,\text{NO}_2\text{-SCR}} \cdot \exp\left(-\frac{E_{\text{A,NO}_2\text{-SCR}}}{R \cdot T}\right) \cdot c_{\text{NO}_2} \cdot \Theta \quad (6)$$

The results show, that there are considerably high amounts of N_2O formed (up to 190 ppm) during this reaction. But as N_2O formation does not play a role for NH_3 dosing control, it is not taken into account here and the stoichiometry between NO_2 and NH_3 is determined empirically. Fig. 7 illustrates simulations and experimental results. There are deviations below 200 °C as in this region NH_4NO_3 formation occurs, which is not implemented in the model.

3.1.6. Standard SCR Reaction

According to the Standard SCR Reaction equimolar amounts of NH_3 and NO react with oxygen to form nitrogen and water (R6).

$$4NH_3 + 4NO + O_2 \rightarrow 4N_2 + 6H_2O \quad (R6)$$

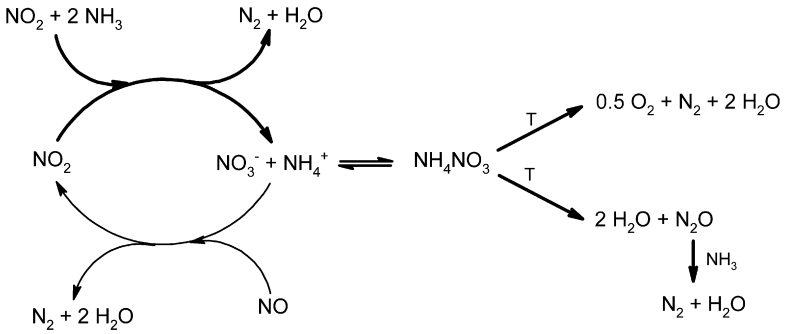

Fig. 6. Mechanism, which can explain the deviant converted amounts of NO_2 and NO during Fast SCR Reaction. Drawn in black the mechanism published by Grossale et al. [24].

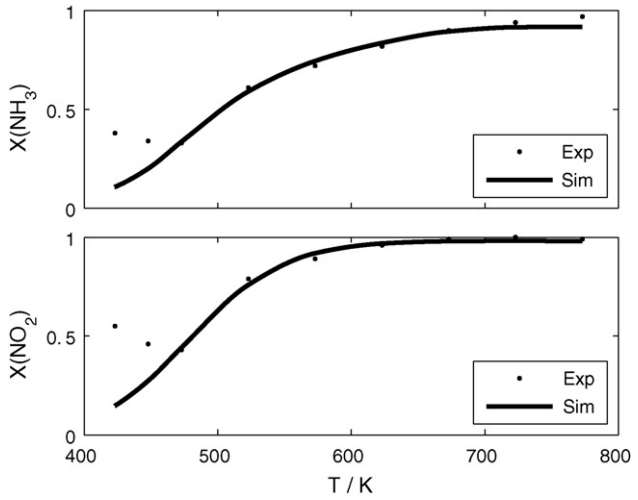

Fig. 7. Simulation and experimental results of the NO_2 SCR Reaction (450 ppm NO_2, 600 ppm NH_3, 6% O_2, 5% H_2O, GHSV 50,000 h^{-1}).

The influence of different O_2 concentrations was investigated in steady state experiments performed at temperatures between 150 and 500 °C, with concentrations of O_2 between 3 and 21% and fixed NO and NH_3 concentrations of 600 ppm (5% H_2O, 6% O_2). The results show, that oxygen promotes the reaction and has an effect on the performance of the catalyst.

The effect of the ammonia concentration was observed in transient response experiments, where an ammonia pulse was applied to a constant feed of NO, the system answer revealed an inhibition of the SCR reaction by NH_3 [13]. An inhibition effect of NH_3 in the Standard SCR Reaction was seen before on Fe_2O_3 catalysts by Willey et al. [25]. For the model parameterization, the impact of the ammonia concentration was studied by reducing α, the dosing ratio of NH_3/NO, stepwise. The effect of the ammonia inhibition arises also in the NO conversion at steady state conditions (Fig. 8). The rate expression for the Standard SCR Reaction, which takes into account both the ammonia inhibition and the impact of the oxygen concentration, is shown in (7):

$$r_{NO} = k_{0,NO} \cdot \exp\left(-\frac{E_{A,NO}}{R \cdot T}\right) \cdot \frac{c_{NO} \cdot \Theta}{1 + K_{NH_3} \cdot \Theta/(1-\Theta)} \cdot \left(\frac{x_{O_2}}{0.06}\right)^{\beta} \quad (7)$$

This expression regards NO as a gaseous reacting species. The inhibition by NH_3 is accounted for by the denominator. The influence of the oxygen concentration is covered by a power law factor. This rate expression has been found to be useful for vanadia-based catalysts by Chatterjee et al. [10]. Simulation results and experiments in terms of the influence of the oxygen concentration are shown in Fig. 9, the results in terms of variation of α are shown in Fig. 10.

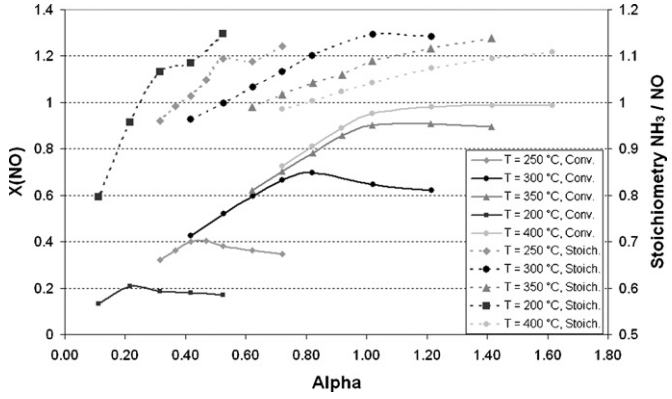

Fig. 8. Conversion and stoichiometry observed during the variation of α, the dosing ration of NH_3 and NO (600 ppm NO and NH_3, 5% H_2O, GHSV 25,000 h^{-1}).

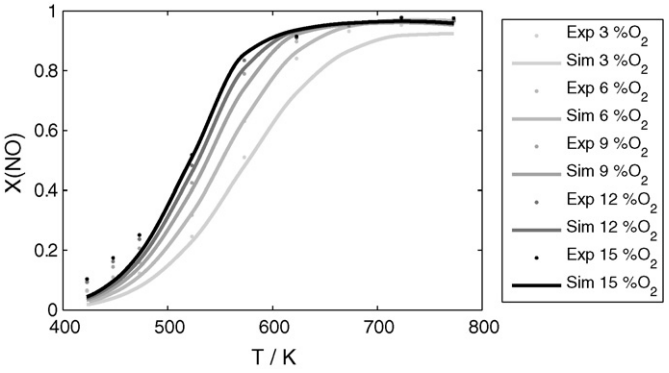

Fig. 9. Simulation and experimental results of the Standard SCR Reaction performed at different O_2 concentrations (3–15% O_2, 600 ppm NO and NH_3, 5% H_2O, GHSV 25,000 h^{-1}).

An important feature of the Standard SCR Reaction on Fe zeolite systems is the stoichiometric ratio of the converted amounts of NH_3:NO. This is not under all conditions 1:1 as predicted in (R6). Dependent on the excess of ammonia provided we observed different stoichiometries. Fig. 8 shows, apart from the NO_x conversions, the stoichiometries of converted amounts of NH_3 and NO during the variation of α. The stoichiometry is a function of α and rises with the excess of ammonia. At the values of α, where the optimum conversion of NO is reached, the stoichiometry of NH_3/NO is above 1 for every temperature. Especially at medium temperatures around 250–350 °C, we see a significant higher ammonia conversion (up to 12% more) as actually needed to reduce the converted NO. This stoichiometry is taken into account in the model empirically. The mechanistic reasons behind this observation are not fully understood. The NH_3 oxidation by O_2 is not the reason for this, as this reaction in this system does not occur until 400 °C. Probably there is a surface species formed during the Standard SCR process, passing through a redox cycle, that consumes NH_3 for the reduction process and O_2 for the oxidation, so that in sum a NH_3 oxidation is observed. The stoichiometry rises with the excess of NH_3, because the redox cycle competes with the Standard SCR process for the adsorbed ammonia. The mechanistic nature of the proposed redox cycle remains unclear. The key step of the Standard SCR Reaction on Fe zeolites is supposed to be an NO oxidation process [8,26]. There

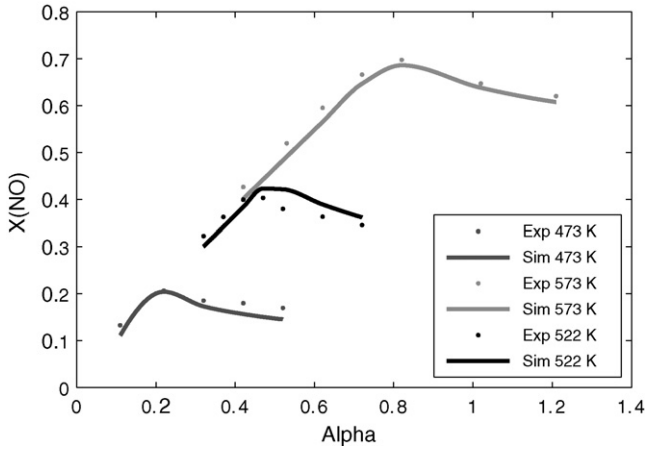

Fig. 10. Simulation and experimental results of the α (the dosing ration of NH_3 and NO) variation during Standard SCR Reaction (600 ppm NO, 6% O_2, 5% H_2O, GHSV 25,000 h^{-1}).

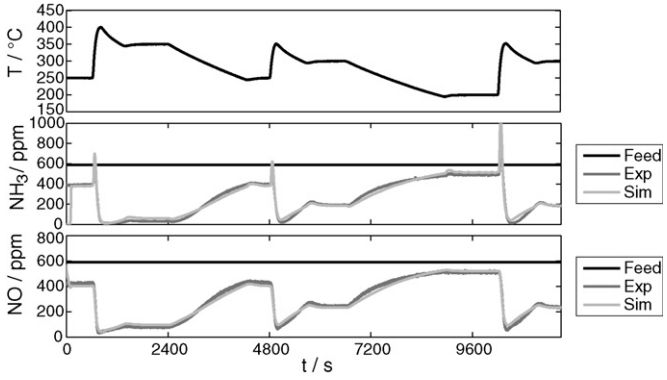

Fig. 11. Temperature profile for model validation (600 ppm NH_3, 600 ppm NO, 6% O_2, 5% H_2O, GHSV 25,000 h^{-1}).

were different NO/O_2 adsorbing species observed at temperatures between 200 and 400 °C [6]. As these are species just occurring with NO_x in the feed gas, they are potentially involved in the proposed redox cycle.

3.2. Model validation

A temperature programmed test procedure was chosen for model validation. In the first step the NO and NH_3 feed concentrations were kept constant (600 ppm NO and NH_3, 6% O_2, 5% H_2O). This experiment should test the model in terms of covering transient temperature conditions, which will also be the challenge in the vehicle. In Fig. 11 the temperature profile is illustrated and simulation and test results are compared. The model well reproduces the steady state conversion levels of NO and NH_3. Also the dynamic features of the system are covered well. On the one hand the impact of temperature overshoots is well reproduced in the conversion curves and on the other hand the ammonia peaks, which arise during temperature gradients, are well reflected. This is especially important, as it is the challenge of the ammonia controller to eliminate these peaks.

3.3. Ammonia dosing control

3.3.1. Setup of the ammonia dosing controller

The scheme of the applied NH_3 dosing controller is illustrated in Fig. 12. It is a feed forward controller, the amount of NH_3 to be dosed is calculated relative to the actual NO inlet concentration, therefore the variable to be determined is α (ratio of NH_3 to NO). The controller can be divided in two units, each depending on a set of lookup tables. The first unit is represented by the upper box in Fig. 12 and accounts for steady state operation. α_{opt}, the optimum value of α, which depends on process parameters like temperature, NO concentration and space velocity, is determined. The second unit, represented by the lower box in Fig. 12, accounts for the ammonia storage level compensation and determines the optimum storage level Θ_{opt}. To be able to compensate transient changes in the input, especially temperature variations, an observer for the NH_3 storage level is implemented. This observer, the calculated relative storage level $\hat{\Theta}$, is compared to the optimum storage level Θ_{opt}, that was derived using steady state simulations for the given inputs. The resulting error $\Delta\Theta$ leads to a compensation of the NH_3 input concentration.

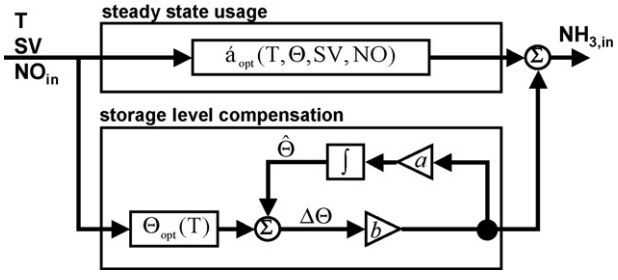

Fig. 12. Scheme of the NH_3 dosing feed forward controller.

The amount of corrected NH_3 feed is also used for the estimation of the actual value of the observer. The relative NH_3 storage level $\hat{\Theta}$ is calculated by integration of the change of the relative NH_3 storage amount (ratio of the amount of corrected NH_3 and the parameter a, the total capacity of the NH_3 storage on the surface). The performance of the feed forward controller is influenced by the control parameter b, which defines how fast the controller zeros the error.

3.3.2. Parameterization

The parameterization of the controller, that means the determination of lookup tables used by the controller, is done by computer simulations based on the NH_3-SCR model. This reduces experimental effort, notably because there are dependencies of the storage level involved. These can be determined by experiments, but the measurements are complex and time consuming. The parameterization is performed based on three criteria:

1. NO conversion criterion: maximum NO conversion has to be achieved.
2. NH_3 slip criterion: maximum NH_3 slip, which is accepted at steady state conditions.
3. NH_3 peak criterion: maximum accepted height of the NH_3, which emerges after the highest temperature gradient expected.

Each of these criteria is described in more detail in the following.

NO conversion criterion: The main goal of the SCR with NH_3 is to minimize the NO output concentration. Because of the inhibition of the Standard SCR Reaction (R6) by NH_3, more NH_3 at the input does not necessarily mean better NO conversion. The NO conversion has a maximum at a certain NH_3 input concentration. This leads to $\alpha_{conv.}$, the α for maximum NO conversion

NH_3 slip criterion: One main challenge in SCR after treatment is the breakthrough of NH_3 at the outlet of the catalyst which should be kept under a certain limit. In this paper we aimed for a maximum NH_3 slip of 10 ppm at steady state conditions. The NH_3 slip is a direct function of the NH_3 storage level and thus of the NH_3 dosing ratio. The dosing ratio, which satisfies this criterion, is named α_{slip}.

NH_3 peak criterion: There are also some dynamic limitations that need to be considered. With increasing temperature, the NH_3 storage capacity decreases and NH_3 from the surface desorbs into the gas phase. This additional amount of NH_3 can be very large and can overcome the total need of NH_3 for the reduction of NO. In this case the resulting NH_3 peak cannot be avoided even if the NH_3 injection is stopped immediately. To prevent the ammonia slip the steady state NH_3 storage level needs to be adapted to a lower value. To determine the optimum storage level Θ_{opt}, a standard simulation sequence is defined. Starting with the system at steady state SCR conditions (defined by α, NO, T and GHSV) a temperature gradient is applied without further dosing of any reactive components. This gradient should be the maximum expected for the system (here: 50 K min^{-1}). This sequence results in both an elevated NO conversion rate and an NH_3 desorption peak. The height of this peak depends on the amount of NH_3 left on the surface before starting the temperature ramp represented by Θ. To determine Θ_{opt} the maximum NH_3 peak that is tolerated has to be defined (here: 20 ppm). As the storage level Θ_{opt} is a direct function of the applied α, this criterion as well leads to an optimum value of the dosing ratio, it is defined as α_{peak}.

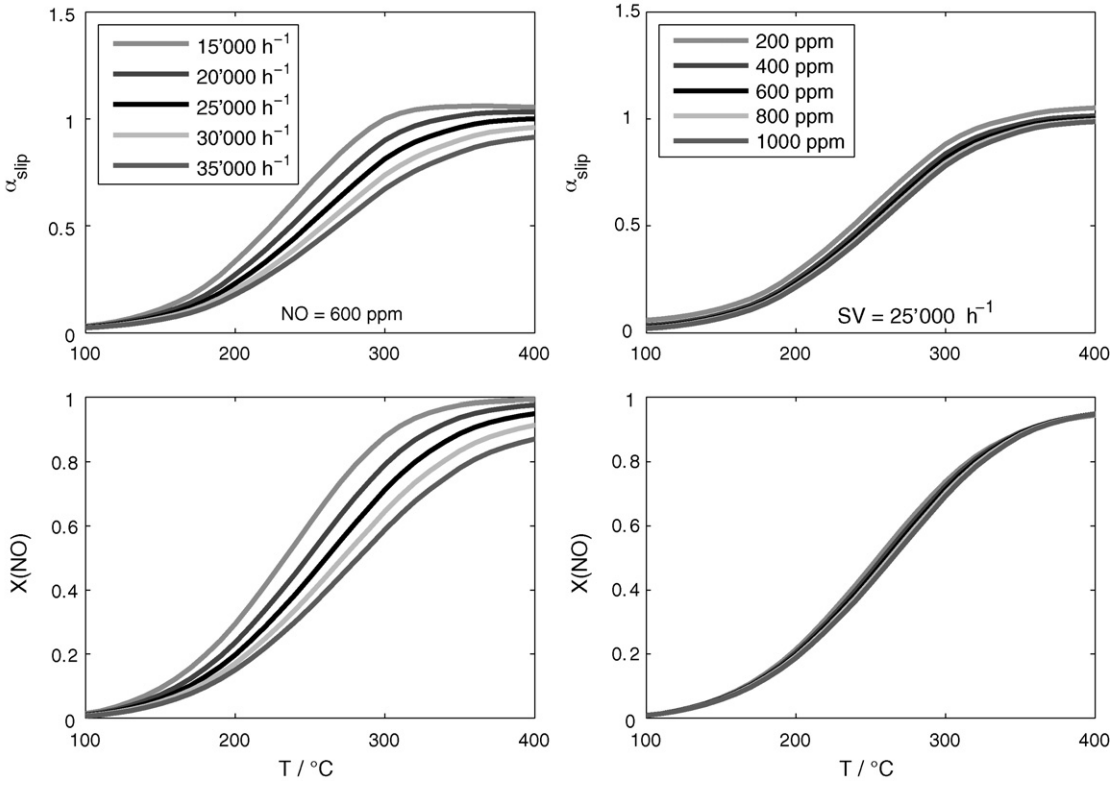

Fig. 13. Effect of different space velocities and NO concentrations, respectively on α_{opt} and NO conversion.

The optimum dosing ratio α_{opt} has to satisfy the three criteria named above. Typically this is the case for the smallest value of the three according like (8) reveals:

$$\alpha_{opt} = \min(\alpha_{conv.}, \alpha_{slip}, \alpha_{peak}) \quad (8)$$

The α for every criterion is a function of different variables, namely temperature, space velocity and NO feed concentration. The temperature of the feed gas has the highest impact on the dosing ratio, but space velocity and NO concentration also have to be considered. As an example the dependencies of α_{slip} determined with the model are shown in Fig. 13. Generally the conversion of NO is small for low temperatures thus only little NH_3 can be used. With decreasing space velocity (plots on the left) the residence time increases leading to a greater α and higher NO_x conversion. The

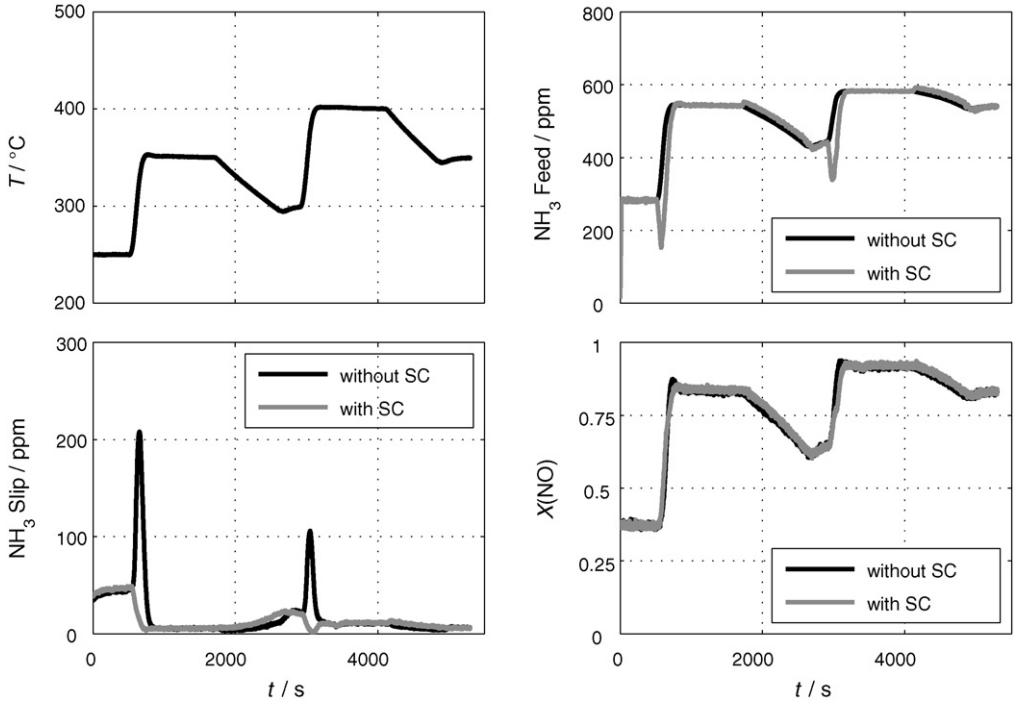

Fig. 14. Validation of the NH_3 dosing controller. In black just with the maps valid for steady state performance, in grey both with maps for NH_3 storage compensation (SC) and steady state performance (600 ppm NO, 6% O_2, 5% H_2O, GHSV 25,000 h^{-1}).

impact of the NO concentration is less eminent, generally a higher NO inlet concentration leads to a lower α_{slip} due to the ammonia inhibition. The lookup tables mapping the optimum dosing ratio α_{opt} for each operation point have to reflect the dependencies mentioned above.

The set of α_{opt} with dependencies of temperature, GHSV and NO concentration results in a three-dimensional lookup table. Since the use of multidimensional lookup tables is computationally costly, some dependencies need to be resolved, so that lower dimensional lookup tables can be used. This is possible, as shown in [14] because the correlation between the space velocity and the NO concentration is weak. Thus, α_{opt} can be mapped by a set of two 2D-lookup tables according to (9).

$$\alpha_{opt} = g(T, SV) \cdot h(T, [NO]_{in}) \quad (9)$$

The lookup table for the storage level compensation is just one 1D-map as the optimum storage level Θ_{opt} is only a function of the temperature.

Although the model is capable of simulating NO_2 concentrations, in a first step only NO was considered for the development of the controller. However, the parameterization proceeds identically when NO_2 is included.

3.3.3. Test of the NH_3 dosing controller at the synthetic gas test bench

The derived controller was parameterized, implemented at the synthetic gas test bench (see Section 2.1) and tested by a temperature programmed test sequence. Two kinds of controllers were implemented on the synthetic gas test bench: one using just the lookup tables for the steady state dosing (the upper box in Fig. 12), and another with the additional storage level compensation (the lower box in Fig. 12). A temperature profile was applied with a constant feed of NO at standard conditions (5% H_2O, 6% O_2, GHSV 25,000 h^{-1}) while the amount of dosed ammonia was determined by the NH_3 dosing controller. In Fig. 14 the results are illustrated. While the controller using only the steady state lookup tables shows considerably high ammonia desorption peaks during temperature rises, these peaks are avoided applying the maps for storage level compensation. Additionally the NH_3 storage compensation has no appreciable effect on the conversion of NO, as illustrated in Fig. 14. This shows that the model-based parameterization of the NH_3 dosing controller works.

4. Conclusions

Within this work we showed the setup of a detailed model for a commercial Fe zeolite catalyst and its use for the parameterization of an NH_3 dosing controller. The model describes the system under steady state as well as under transient conditions. One important mechanistic detail is the inhibition of the Standard SCR Reaction by ammonia, another the stoichiometry during Standard SCR conditions. This characteristic discerns Fe zeolite catalysts from other NH_3-SCR systems, e.g. vanadia-based catalysts. Different amounts of NO/NO_2 converted during the Fast SCR have been observed and to our knowledge are not reported on other systems.

For Standard SCR conditions the model was validated with transient experiments. It was demonstrated, that the model can be used to populate lookup tables for a feed forward NH_3 dosing controller. Finally, the performance of the so parameterized controller is proven in a model gas experiment. Testing of a controller at a synthetic gas test bench allows to test the system in view of catalysis related effects without any interference of urea injection phenomena.

References

[1] L.J. Alemany, L. Lietti, N. Ferlazzo, P. Forzatti, G. Busca, E. Giamello, F. Bregani, Reactivity and physicochemical characterization of V_2O_5–WO_3/TiO_2 De-NOx catalysts, Journal of Catalysis 155 (1) (1995) 117–130.

[2] P. Forzatti, L. Lietti, Recent advances in DeNOxing catalysis for stationary applications, Heterogeneous Chemistry Reviews 3 (1996) 33–35.

[3] M. Iwamoto, H. Furukawa, Y. Mine, F. Uemura, S. Mikuriya, S. Kagawa, Copper(ii) ion-exchanged ZSM-5 zeolites as highly active catalysts for direct and continuous decomposition of nitrogen monoxide, Journal of Chemical Society, Chemical Communications (1986) 1272–1273.

[4] G. Busca, L. Lietti, G. Ramis, F. Berti, Chemical and mechanistic aspects of the selective catalytic reduction of NO_x by ammonia over oxide catalysts: a comment, Applied Catalysis B: Environmental 18 (1998) 1–36.

[5] H.-Y. Chen, W.M.H. Sachtler, Activity and durability of Fe/ZSM-5 catalysts for lean burn NO_x reduction in the presence of water vapor, Catalysis Today 42 (1–2) (1998) 73–83.

[6] R.Q. Long, R.T. Yang, Characterization of Fe–ZSM-5 catalyst for selective catalytic reduction of nitric oxide by ammonia, Journal of Catalysis 194 (1) (2000) 80–90.

[7] R.Q. Long, R.T. Yang, Temperature-programmed desorption/surface reaction (TPD/TPSR) study of Fe-exchanged ZSM-5 for selective catalytic reduction of nitric oxide by ammonia, Journal of Catalysis 198 (2001) 20–28.

[8] R.Q. Long, R.T. Yang, Reaction mechanism of selective catalytic reduction of NO with NH_3 over Fe–ZSM-5 catalyst, Journal of Catalysis 207 (2002) 224–231.

[9] E. Tronconi, I. Nova, C. Ciardelli, D. Chatterjee, B. Bandl-Konrad, T. Burkhardt, Modelling of an SCR catalytic converter for diesel exhaust after treatment: dynamic effects at low temperature, Catalysis Today 105 (3-4) (2005) 529–536.

[10] D. Chatterjee, T. Burkhardt, M. Weibel, Numerical Simulation of $NO/NO_2/NH_3$ reactions on SCR-catalytic converters, SAE (2006), 2006-01-0468.

[11] D. Chatterjee, T. Burkhardt, M. Weibel, I. Nova, A. Grossale, E. Tronconi, Numerical simulation of zeolite- and V-based SCR catalytic converters, SAE (2007), 2007-01-1136.

[12] C.M. Schär, C.H. Onder, H.P. Geering, Control-oriented model of an SCR catalytic converter system, SAE (2004), 2004-01-0153.

[13] S. Malmberg, M. Votsmeier, J. Gieshoff, N. Soeger, L. Mussmann, A. Schuler, A. Drochner, Dynamic phenomena of SCR-catalysts containing Fe-exchanged zeolites—experiments and computer simulations, Topics in Catalysis 42–43 (1) (2007) 33–36.

[14] A. Schuler, M. Votsmeier, S. Malmberg, J. Gieshoff, A. Drochner, G. Vogel, P. Kiwitz, Dynamic model for the selective catalytic reduction of NO with NH_3 on Fe–zeolite catalysts, SAE (2008), 2008-01-1323.

[15] L. Olsson, H. Sjövall, R.J. Blint, A kinetic model for ammonia selective catalytic reduction over Cu–ZSM-5, Applied Catalysis B: Environmental 81 (3–4) (2008) 203–217.

[16] F. Willems, R. Cloudt, E. van den Eijnden, M. van Genderen, R. Verbeek, B. de Jager, W. Boomsma, I. van den Heuvel, Is closed-loop SCR control required to meet future emission targets? SAE (2007), 2007-01-1574.

[17] M. Devarakonda, G. Parker, J.H. Johnson, V. Strots, S. Santhanam, Adequacy of reduced order models for model-based control in a urea-SCR after treatment system, SAE (2008), 2008-01-0617.

[18] M. Shost, J. Noetzel, M.-C. Wu, T. Sugiarto, T. Bordewyk, G. Fulks, G.B. Fisher, Monitoring, feedback and control of urea SCR dosing systems for NO_x reduction: utilizing an embedded model and ammonia sensing, SAE (2008), 2008-01-1325.

[19] E. Tronconi, L. Lietti, P. Forzatti, S. Malloggi, Experimental and theoretical investigation of the dynamics of the SCR—DeNOx reaction, Chemical Engineering Science 51 (1996) 2965–2970.

[20] W. Hauptmann, A. Drochner, H. Vogel, M. Votsmeier, J. Gieshoff, Global kinetic models for the oxidation of NO on platinum under lean conditions, Topics in Catalysis 42-43 (1) (2007) 157–160.

[21] M. Schwidder, S. Heikens, A. De Toni, S. Geisler, M. Berndt, A. Brückner, W. Grünert, The role of NO_2 in the selective catalytic reduction of nitrogen oxides over Fe–ZSM-5 catalysts: active sites for the conversion of NO and of NO/NO_2 mixtures, Journal of Catalysis 259 (1) (2008) 96–103.

[22] A. Grossale, I. Nova, E. Tronconi, Study of a Fe–zeolite-based system as NH_3-SCR catalyst for diesel exhaust after treatment, Catalysis Today 136 (2008) 18–27.

[23] A. Grossale, I. Nova, E. Tronconi, D. Chatterjee, M. Weibel, The chemistry of the NO/NO_2-NH_3 "fast" SCR reaction over Fe–ZSM5 investigated by transient reaction analysis, Journal of Catalysis 256 (2) (2008) 312–322.

[24] M. Devadas, O. Kroecher, M. Elsener, A. Wokaun, N. Soeger, M. Pfeifer, Y. Demel, L. Mussmann, Influence of NO_2 on the selective catalytic reduction of NO with ammonia over Fe–ZSM5, Applied Catalysis B: Environmental 67 (3–4) (2006) 187–196.

[25] R.J. Willey, J.W. Eldridge, J.R. Kittrell, Mechanistic model of the selective catalytic reduction of nitric oxide with ammonia, Industrial & Engineering Chemistry Product Research and Development 24 (1985) 226–233.

[26] M. Devadas, O. Kroecher, M. Elsener, A. Wokaun, G. Mitrikas, N. Soeger, M. Pfeifer, Y. Demel, L. Mussmann, Characterization and catalytic investigation of Fe–ZSM5 for urea-SCR, Catalysis Today 119 (1–4) (2007) 137–144.

[27] B. Coq, M. Mauvezin, G. Delahay, J.-B. Butet, S. Kieger, The simultaneous catalytic reduction of NO and N_2O by NH_3 using an Fe-zeolite-beta catalyst, Applied Catalysis B: Environmental 27 (2000) 193–198.